Mon. Not. R. Astron. Soc. **277**, 641–654 (1995)

Neutral hydrogen studies of the Seyfert galaxy NGC 3227

C. G. Mundell,[1] A. Pedlar,[1] D. J. Axon,[1,2] J. Meaburn[3] and S. W. Unger[4]

[1] *University of Manchester, Nuffield Radio Astronomy Laboratories, Jodrell Bank, Macclesfield, Cheshire SK11 9DL*
[2] *Affiliated to Space Science Division of ESA, Space Telescope Science Institute, 3700 San Martin Drive, Baltimore MD21218, USA*
[3] *Department of Physics and Astronomy, University of Manchester, Oxford Road, Manchester*
[4] *Royal Greenwich Observatory, Madingley Road, Cambridge CB3 0EZ*

Accepted 1995 June 16. Received 1995 June 9; in original form 1995 February 27

ABSTRACT

We have used the VLA to image the neutral hydrogen emission from the Seyfert galaxy NGC 3227, with angular resolutions ranging from 12 to 60 arcsec. We detect plumes of H I extending to ~70 kpc north and ~31 kpc south of the galaxy which may be a consequence of interaction. Complex motions in the galactic disc have been resolved into emission from the disc, which is in approximate solid body rotation, and an anomalous velocity cloud, situated north-west of the disc at the base of the northern plume. The cloud has a mean velocity of ~150 km s^{-1} above the systemic velocity of NGC 3227 and shows evidence of rotation. We suggest that this cloud is a gas-rich dwarf galaxy that either is one of the bodies responsible for the interaction, or has formed as a consequence of the interaction.

No neutral hydrogen emission is associated with the companion galaxy NGC 3226, and the presence of low velocity (500 km s^{-1}) gas reported in single dish measurements is not detected in the present observations.

The continuum image of NGC 3227 shows an extended component, in addition to the compact core, that may be enhanced disc emission due to the interaction. In the central 15 arcsec of the disc we detect evidence of H I absorption against the nuclear continuum source. Higher resolution observations are required to confirm this.

Although the velocities in the disc are remarkably close to solid body velocities (considering the presence of a disturbing companion), the integrated neutral hydrogen emission shows a bar of enhanced emission crossing the nucleus, in a north-west to south-east direction, that has a 'Z' shaped morphology and trails in the same sense as the optical spiral arms. This H I bar seems to be a continuation of the CO bar and we suggest that it may play an important role in the fuelling of the AGN.

From our H I observations we deduce a heliocentric systemic velocity of 1135 ± 10 km s^{-1} for NGC 3227. We derive a value of 56° for the inclination of the galactic disc and $158° \pm 2°$ for the PA of the major axis. Neutral hydrogen masses of 5.7×10^8 $M_\odot$ for the disc, 2.1×10^8 $M_\odot$ for the cloud, 1.3×10^8 $M_\odot$ in the southern plume and 1.8×10^8 $M_\odot$ in the northern plume were found, resulting in a total H I mass for NGC 3227 of 1.1×10^9 $M_\odot$.

Key words: galaxies: individual: NGC 3227 – galaxies: interactions – galaxies: Seyfert – radio lines: galaxies.

1 INTRODUCTION

In order to 'fuel' an active galactic nucleus (AGN), gas must be delivered to the centre of the galaxy, with essentially zero angular momentum and the actual delivery rate of the gas on to the central object is regulated by the formation of an accretion disc, which collects the infalling gas (Osterbrock 1991). It has been suggested that tidal interactions between galaxies play a key role in this process, providing not only a way to trigger nuclear activity and starburst phenomena, but also rejuvenating dormant AGNs (Barnes & Hernquist 1992). During an interaction, gas can be supplied to the nucleus in two ways: either directly, when gas from the companion, or outer regions of the active galaxy, is tidally

removed and deposited on to the nucleus; or by instabilities (such as bars) which produce non-circular motions and inflows of the galactic gas, due to gravitational perturbations of the orbits near the nucleus (Shlosman 1989).

Seyfert galaxies represent the low luminosity end of the AGN phenomenon, but are the closest, most common class of active galaxy (present in ~2 per cent of field galaxies). Adams (1977), Simkin, Su & Schwarz (1980), Heckman (1978) and others found that many Seyfert galaxies are distorted spirals, are barred, have nearby 'companion' galaxies, or are in pairs or interacting systems. Various statistical studies (Dahari 1984, 1985; MacKenty 1989, 1990; Keel 1985) suggest that Seyfert galaxies are more likely to have companions than 'normal' (non-Seyfert) galaxies. It is interesting to note that, although interacting galaxies tend to have an excess of AGN, *strongly* interacting systems do not (Bushouse 1986; Osterbrock 1991 and references therein).

Neutral hydrogen is often the most spatially extended, observable component of a galaxy's disc and so is expected to be sensitive to interactions (Gallagher, Knapp & Faber 1981). Disruptive encounters between galaxies with small relative velocities often cause tidal effects, producing bridges and tails of H I extending out to several galaxy diameters (Haynes, Giovanelli & Chincarini 1984). Observations of H I are, therefore, particularly important when studying interacting galaxies as the neutral gas may be used as a 'tracer' of a galaxy's response to an interaction.

NGC 3227 is a striking example of a nearby Seyfert galaxy undergoing an interaction. The host galaxy is classified as an SAB pec and is interacting with the nearby SO or E2 galaxy NGC 3226. Various Seyfert classifications have been assigned to the nucleus in NGC 3227 through the literature, but the presence of a broad line region (Salamanca et al. 1994 and references therein) leads to the classification of NGC 3227 as a type 1 Seyfert.

Rubin & Ford (1968) conducted an extensive optical study of the NGC 3226, 3227 pair. They used long-slit spectroscopy to study the kinematics of the excited gas in the system, finding evidence of gas outflow from the nucleus. They also detected an 'arm', stretching from NGC 3227 to its companion, with a mean velocity of 550 km s^{-1}.

Blitz, Mathieu & Bally (1986) detected CO(J = 1–0) emission, from the system, with a large beam (1.1 arcmin) and Meixner et al. (1990) studied this emission with high resolution observations obtained with the OVRO interferometer. They detected two unresolved peaks, which appear to straddle the optical nucleus in an east–west direction, and a more extended component, approximately 17 arcsec in length, pointing towards the companion galaxy.

Heckman et al. (1978) obtained single-dish observations of the H I emission in the NGC 3226, 3227 system. They used the Aricebo telescope, with a 3.3-arcmin beam, to derive an estimate for the flux integral of 20.0 Jy km s^{-1}. They also suggest the presence of a weak emission wing extending down to 500 km s^{-1}, in the line profile taken 3 arcmin north of the nucleus of NGC 3227.

To date, few H I synthesis studies of AGNs have been published, even though such data provide one of the clearest observational methods of investigating the role of interactions in the fuelling chain.

In this paper we present neutral hydrogen observations of NGC 3227 obtained with the NRAO very large array (VLA) in D and C configurations. Section 2 gives details of the observations and the subsequent reduction of the data, while discussion of the detailed H I distribution and kinematics and continuum emission from the interacting pair is presented in Section 3. Derived quantities such as H I and total masses are also presented in Section 3. The conclusions are presented in Section 4. Throughout we assume $H_0 = 75$ km s^{-1} Mpc^{-1}, which at a heliocentric redshift of 1135 km s^{-1} gives a distance of 15.1 Mpc for NGC 3227, therefore one arcsec corresponds to 73 pc in the galaxy.

2 OBSERVATIONS

2.1 Observations and reduction

We obtain observations, using the VLA in C and D configurations, of NGC 3227 in the 21-cm neutral hydrogen line. Spectral line mode 1A was used for both data sets, with automatic band-pass calibration and on-line Hanning smoothing performed on the C-array data. Data suffering from 'shadowing' (where one antenna's line of sight is obscured by another) were discarded. The observational parameters are detailed in Table 1.

D-array observations used 64 channels over a bandwidth of 12.5 MHz but on-line data handling limitations at the time allowed only the central 32 channels to be recorded, resulting in a channel separation of 41.2 km s^{-1}. As no on-line Hanning smoothing was applied, the spectral resolution was also effectively 41.2 km s^{-1} per channel.

The D-array band was centred at 992 km s^{-1}, rather than the systemic velocity of NGC 3227, in order to accommodate the low velocity feature, reported by Heckman et al. (1978), in the band. Emission from gas at this velocity was, however, not detected in our D-array observations, so the

Table 1. Observing parameters for VLA D- and C-array observations of NGC 3227.

PARAMETER	D Array	C Array
Date of Observations	24 November, 1985	17 May, 1988
Field Centre (1950)	$\alpha = 10^h20^m46^s$ $\delta = 20°07'06''$	$\alpha = 10^h20^m46^s$ $\delta = 20°07'06''$
Central Velocity	~ 992 km s^{-1}	1200 km s^{-1}
No. of Antennae	27	27
Time on Source	6 hours	9.5 hours
Frequency Channels	32	64
Total Bandwidth	6.25 MHz	6.25 MHz
Channel Separation	195.313 kHz	97.656 kHz
Velocity Resolution	41.2 km s^{-1}	25 km s^{-1}
Amplitude Calibrator	3C286	3C286
Phase Calibrator	1005+077	1019+222
Spectral Line Mode	1A	1A (With On-line Hanning Smoothing)
Primary Beam	30′	30′

C-array observations were centred close to the systemic velocity of NGC 3227 at 1200 km s^{-1}.

The two data sets were calibrated in amplitude and phase using 1005+077 and 1019+222 (for D- and C-array respectively), whose amplitudes were determined from observations of 3C286, assuming a flux density of 14.755 Jy at 1415 MHz (Baars et al. 1977).

All data processing was performed using the NRAO astronomical image processing system (AIPS) package. The calibration and initial data editing were carried out on the two data sets separately, using the 'pseudo-continuum' channel (channel 0) which is formed on-line by averaging the central 75 per cent of the band (4.7 MHz).

The resulting phase and gain solutions were applied to the D-array spectral-line data. These data were then Fourier transformed to produce two cubes, one using natural weighting to optimize surface brightness sensitivity, the other uniformly weighted for maximum resolution. The cube dimensions were 512 × 512 × 32, with 15 arcsec pixels.

Continuum images were formed, from the D-array data, by averaging six channels, free of line emission (channels 1–3 and 29–31), in the natural and uniform cubes. Note that these channels are not at the edge of the band as only the central 32 out of 64 channels were used. The continuum images were deconvolved using the CLEAN algorithm (Högbom 1974), to remove side-lobe structure. The images produced from the naturally and uniformly weighted data were restored with effective beams of 60.74 × 58.15 arcsec and 42.97 × 41.49 arcsec half-power full width (FWHM) respectively. The naturally weighted image is shown in Fig. 1(a). The rms noise in the naturally weighted continuum maps is 0.3 mJy $beam^{-1}$.

Similarly, 512 × 512 × 64, naturally and uniformly weighted cubes were produced from the calibrated C-array data, with 5-arcsec cells. Continuum images were formed by averaging 14 channels, free of line emission (channels 8–15 and 50–57; avoiding the channels close to the edges of the band), in the natural and uniform cubes. These naturally and uniformly weighted continuum images were CLEANed and restored with effective beams of 20.47 × 18.25 arcsec and 13.69 × 12.37 arcsec (FWHM) respectively. The uniform continuum map has an rms noise of 0.3 mJy $beam^{-1}$ and can be seen in Fig. 1(b).

The 'dirty' continuum images were then subtracted from their respective cubes to form 'continuum-free' spectral-line cubes.

In the D-array data, the residuals showed emission over the velocity range of 1408 km s^{-1} to 951 km s^{-1} (i.e. channels 7 to 18), with an rms noise per channel of 0.5 mJy $beam^{-1}$. The residuals in the C-array data showed emission over the range 1325 km s^{-1} to 888 km s^{-1} (channels 26 to 47) with an rms noise per channel of 0.5 mJy $beam^{-1}$. Each of the channels were CLEANed and restored with the same beams as the corresponding continuum images.

Altogether the resolution of the uniformly weighted data is higher than that of the naturally weighted data, the signal-to-noise ratio is degraded; therefore the subsequent analysis was performed, mainly, on the naturally weighted data.

Linear slopes in the baselines, which were visible where significant continuum emission was present, were removed by subtracting linear baseline fits to channels 8 to 15 (corresponding to a velocity range of 1699 km s^{-1} to 1553 km s^{-1}) and 50 to 57 (i.e. 826 to 681 km s^{-1}). The effect was only noticeable in the central ten pixels.

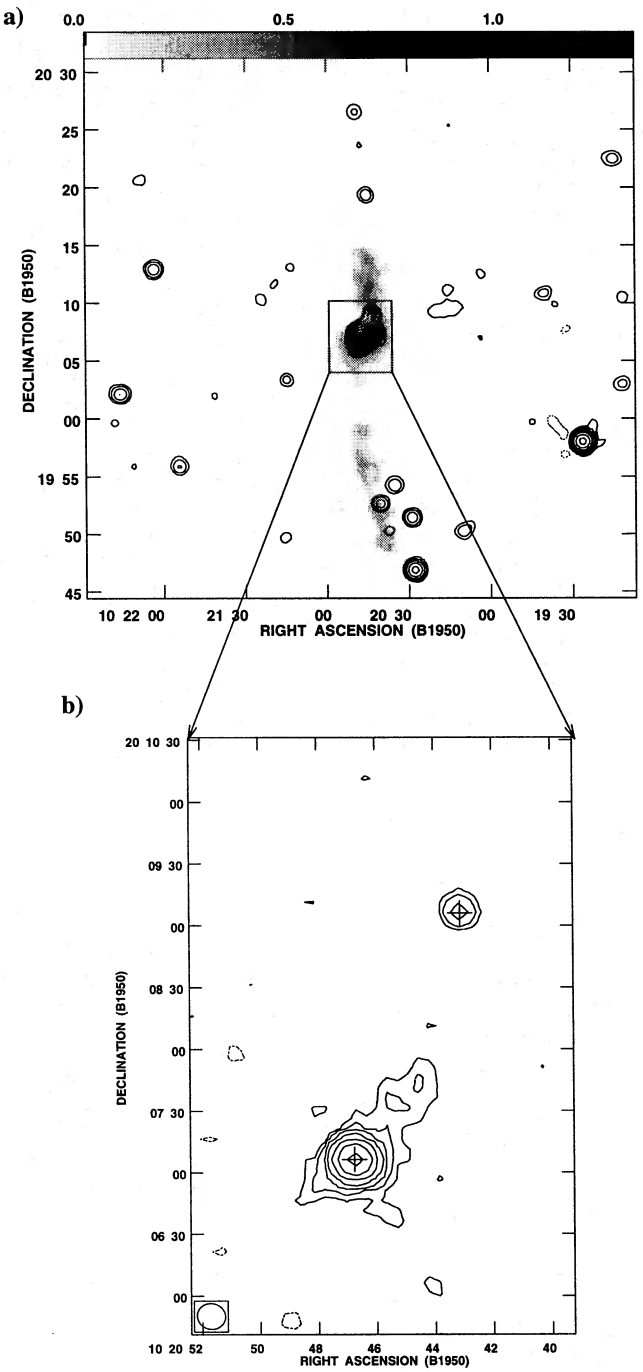

Figure 1. (a) D-array continuum image from the naturally weighted data. Contour levels are (−1.2, 1.2, 2.4, 4.8, 9.6, 19.2, 38.4, 76.8) mJy $beam^{-1}$. The integrated neutral hydrogen distribution of NGC 3227 can also be seen in grey (see Fig. 5). The beam-size is 60.74 × 58.15 arcsec. (b) The uniformly weighted, C-array image with beam-size 13.69 × 12.37 arcsec and contour levels (−1, 1, 2, 4, 8, 16, 32, 64) mJy $beam^{-1}$. The crosses mark the optical positions of NGC 3226 and 3227 (Clements 1981), with the northern component being coincident with the optical position of NGC 3226, and the southern with NGC 3227.

The integrated neutral hydrogen distribution and the corresponding velocity field, were derived from the data by

moment analysis using AIPS task MOMNT. This task smooths the data in both space and velocity and applies a suitable flux cut-off to prevent the inclusion of noise from corrupting the analysis. We performed the profile analysis by smoothing in velocity, using a Hanning smoothing function with convolution cell size 5, and spatially, with a Gaussian function with cell size 3. Only emission greater than 0.8 mJy beam^{-1} was included in the integration. A reduction in this flux cut-off level to 0.6 mJy beam^{-1} showed the presence of regions of weaker emission but systematic errors in the velocity field were produced when this cut-off level was used in the moment analysis.

After the baseline slopes were removed, there appeared to be an absence of H I emission in this region. It was not clear, by simply examining the emission spectra whether absorption, against the continuum source, was present. Therefore, the average emission, *excluding* the central CLEAN-beam area, was subtracted. This average spectrum was formed from the spectra in the 16 pixels surrounding a 3×3 pixel grid, centred on the brightest continuum pixel. We then subtracted this mean spectrum from the central pixel to form the absorption spectrum. Several averaging schemes were tried and all showed some absorption.

The absence of lower order spacings mean that the present observations are insensitive to extended structure larger than 5 arcmin for C-array and 15 arcmin for D-array.

3 RESULTS

3.1 21-cm continuum images

The CLEANed continuum images from the naturally weighted D-array data and the uniformly weighted C-array data are shown in Fig. 1. As can be seen from the lower resolution D-array map, the continuum image consists of ~15 background sources, with a double source at the centre of the image. At C array, this double is clearly resolved into the southern source, which is coincident with the (optical) nucleus of NGC 3227 and the northern source, with the optical position of NGC 3226. The continuum image shown in Fig. 1(b) is a subimage in the vicinity of NGC 3227. The optical positions (Clements 1981) are marked with crosses on the map.

In addition to the compact emission from the core of NGC 3227, a weaker, extended component can be seen, pointing in a north-west direction (Fig. 1b). This extended component is most likely to be disc emission that has been enhanced by the interaction [similar to the extended continuum emission detected in other interacting systems such as Stefan's Quintet (van der Hulst & Rots 1981)], rather than collimated emission or a 'jet'. In fact, high-resolution observations (Mundell et al. 1995b) have shown the PA of the nuclear collimated ejection to differ from this diffuse component by ~30°. The measured positions and total fluxes of NGC 3226 and 3227 can be seen in Table 2. The total flux of NGC 3227 of 99.4 ± 5.6 mJy compares well with Edelson's (1987) measurement of 101.0 ± 5.5 mJy at 20 cm.

Table 2. Measured positions and fluxes of the continuum emission from NGC 3226 and 3227 (from the uniformly weighted C-array data).

	NGC3226	NGC3227
RA (B1950)	$10^h20^m43.11^s$	$10^h20^m46.74^s$
Dec (B1950)	20° 09′ 6.98″	20° 07′ 6.23″
Total Flux Density (mJy)	4.5 ± 0.8	99.4 ± 5.6

3.2 Overview of H I emission

The single-dish estimate for the flux integral of 20.0 Jy km s^{-1} (Heckman et al. 1978) agrees well with our value of 18.3 Jy km s^{-1} obtained from the D-array data (our value is slightly lower than the single-dish estimate, probably arising from missing short spacings). The general shape of the single-dish spectrum is also similar to ours, but we *do not* detect (at an upper limit of 1.5 mJy) the low-velocity gas at 500 km s^{-1} reported by Heckman et al. (1978). This non-detection might be explained by the lack of short spacings (as discussed in Section 2.1). Its presence in the single-dish spectrum, however, could arise from baseline uncertainties in the Arecibo data.

In the continuum-subtracted D-array cube, H I emission was visible in channels 7 to 18 (1408 to 951 km s^{-1}). This residual emission can be seen in the naturally weighted, CLEANed, channel maps shown in Fig. 2. No H I emission is present, above the rms noise level of 0.5 mJy beam^{-1}, in any of the other planes in the cube. As can be seen from the individual channel maps, the H I consists of two plumes of emission, extending approximately north and south, in addition to the central concentration.

There is also much H I associated with the central region of NGC 3227, but, at D-array resolution, the emission appeared to be complex, with many pixels exhibiting multiple component Gaussian features (Fig. 3). This occurs because emission from different regions of gas (moving with different velocities), appears within the large D-array beam.

The C-array observations, however, showed that the emission from the central region of NGC 3227 is, in fact, less complex than indicated by the D-array data. The improved spatial resolution provided by the C array (a factor of 3 better than at D array) was sufficient to resolve the regions of gas moving with different velocities, so that only single Gaussian velocity components were present in each pixel. This allowed us to perform moment analysis with some confidence.

Neutral hydrogen emission was found in channels 26 to 47 (1325–888 km s^{-1}) in the C-array cubes, and the channel maps from the naturally weighted cube are shown in Fig. 4. The C-array observations reveal the presence of an anomalous velocity cloud in addition to the emission from the disc of the galaxy. The cloud is visible, as the upper component, in channels 26 (1325 km s^{-1}) to 35 (1138 km s^{-1}) and is most obvious in channel 29. Fig. 4 also has the optical positions of NGC 3226 and 3227 marked as crosses '+'. Weak evidence of the plumes, seen at D array, is also evident in the C-array data but not shown here.

Although NGC 3226 is positioned at the base of the northern plume, as can be seen in Fig. 2 it should be noted that the improved resolution of the C-array data (Fig. 4) clearly shows that there is no H I associated with NGC 3226 (to an upper limit of 1.5 mJy).

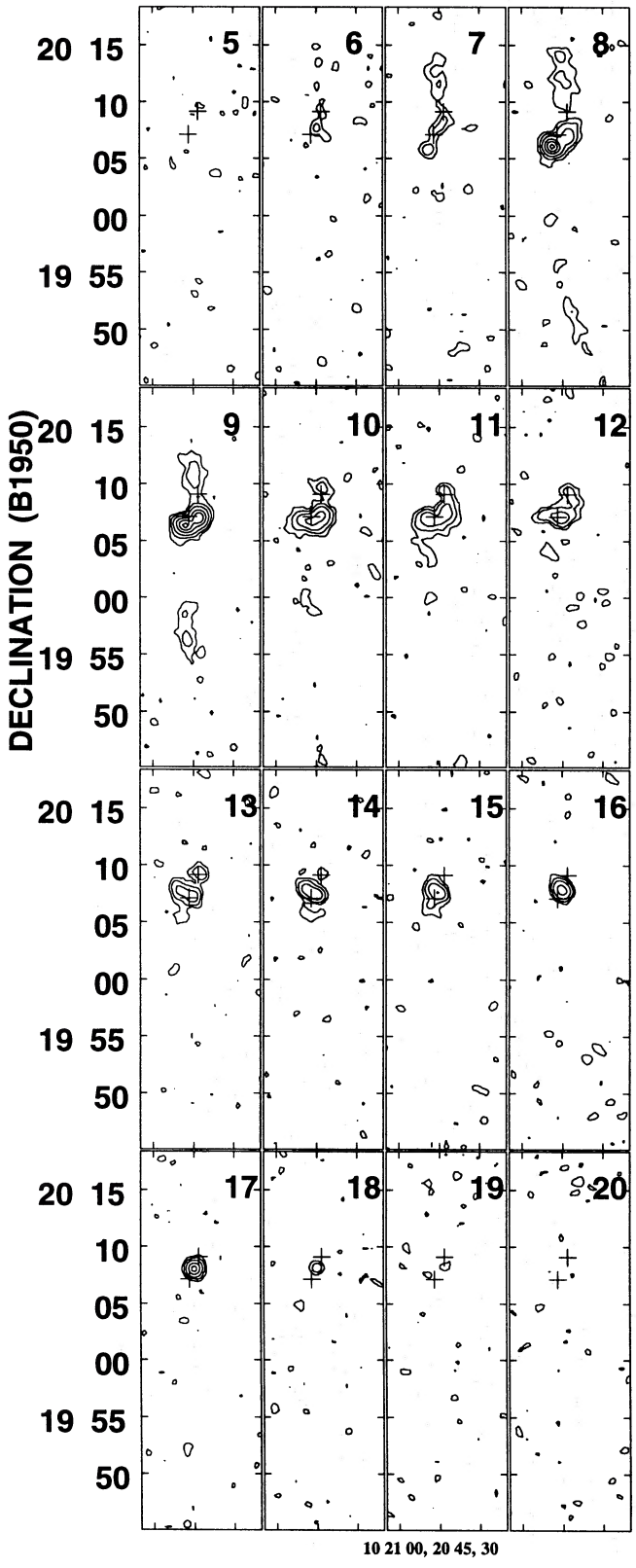

Figure 2. D-array channel maps. Channel 5 corresponds to a velocity of 1491 km s^{-1} and each channel decreases by 41.2 km s^{-1}. The contour levels are (-1.3, 1.3, 2.6, 5.2, 10.4, 15.6, 20.8) mJy beam^{-1} where 1 mJy beam^{-1} corresponds to a column density of 1.32×10^{19} cm^{-2} in each channel. The beam size is 60.74×58.15 arcsec. The optical positions of NGC 3226 and 3227 are marked with '+'; NGC 3226 is the northern '+'.

3.3 The plumes – evidence for interaction?

The D-array observations reveal relatively low surface brightness emission from two large plumes of neutral hydrogen, extending ~31 kpc north and ~70 kpc south of the NGC 3226, 3227 system. The plumes can be seen most effectively in the integrated neutral hydrogen emission image shown in Fig. 5. A primary beam correction was applied to this map to compensate for the antenna beam attenuation at the edge of the field. Channels 5 to 11 only were used in the moment analysis, to emphasize the weak emission from the plumes, so that not all of the emission from the centre of the galaxy is included. The range in velocity along the plumes is evident from the channel maps in Fig. 2.

It can be seen, from Fig. 5, that there is a lack of symmetry between the two plumes, with the southern plume being significantly narrower and more elongated than the northern plume. The northern plume also exhibits a larger spread in velocity as is illustrated in Fig. 6. Taken in conjunction, these two facts suggest that the northern plume has suffered a greater disturbance than the southern plume.

The peak value of column density in the northern plume is 3.9×10^{20} cm^{-2} and in the southern plume is 9.2×10^{19} cm^{-2}. The lowest detectable column density is 2.0×10^{19} cm^{-2}. The average values of column density (averaged over the observed extent of each plume) are 7.0×10^{19} cm^{-2} and 3.4×10^{19} cm^{-2} for the northern and southern plume respectively, giving corresponding neutral hydrogen masses of 1.8×10^{8} $M_\odot$ and 1.3×10^{8} $M_\odot$.

There are many well-studied examples of galaxy interactions and mergers producing tidal plumes and bridges of gas [for example NGC 3628 (Rots 1978), NGC 4038, 4039 (Schweizer 1978; van der Hulst 1979), NGC 4676 (Dahari 1985), NGC 7252 (Schweizer 1978; Hibbard et al. 1994) and NGC 7715 (Smith & Wallin 1992)]. Tidal models, such as those presented by Toomre & Toomre (1972), have successfully reproduced many of the features (like bridges and tails) that are indicative of interactions. They (Toomre & Toomre 1972) demonstrated that tidal features between interacting galaxies could be produced by gravitational forces alone (without the need to include e.g. electromagnetic forces, to form narrow tails), with the most dramatic effects occurring for a direct encounter where the companion's angular velocity temporarily matches that of the disc. The absence of strong continuum emission from tails also implies that magnetic forces do not play a major role (van der Hulst 1979).

The plumes in NGC 3227 confirm that an interaction is taking place and that NGC 3226 (situated at the base of the northern plume) is a possible candidate for the disturbing galaxy. Work is in progress to model the interaction between NGC 3226 and 3227 and will be presented in a later paper (Mundell & Wilkinson, in preparation).

3.4 The anomalous feature – cloud or dwarf galaxy?

If we follow the northern plume of NGC 3227 into the galaxy, we see an anomalous feature that is not associated with disc rotation. The cloud is the upper component, visible in channels 26 to 35 (see Fig. 4).

The position–velocity diagram, in Fig. 7, was formed by summing the emission parallel to the major axis along PA ~158°. The anomalous velocity cloud is clearly visible centred at ~1250 km s^{-1}.

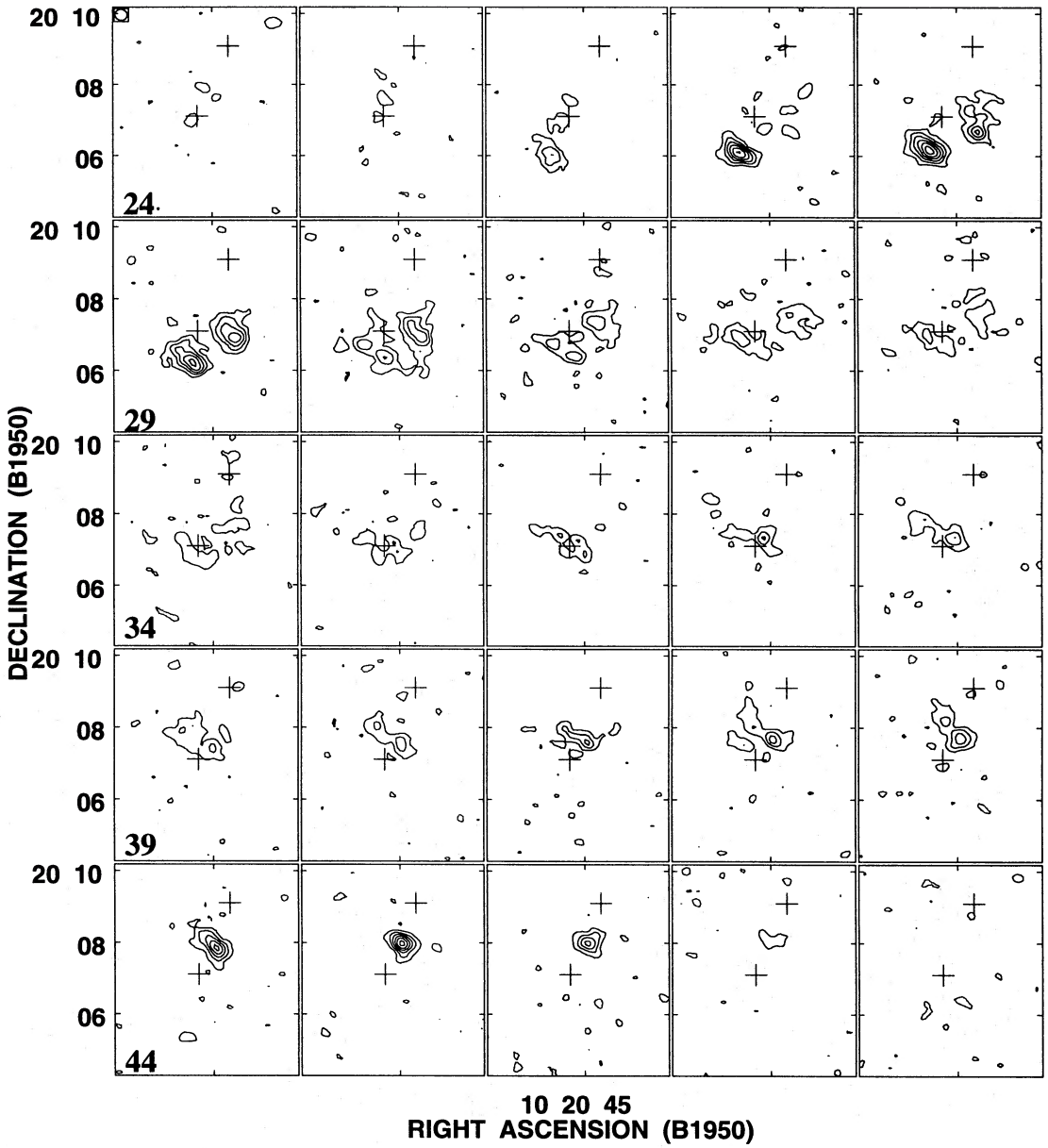

Figure 4. C-array channel maps (channel 24 corresponds to a velocity of 1366 s^{-1}, 48 corresponds to 868 km s^{-1} and each channel is separated by 20.6 km s^{-1}), from the naturally weighted data, showing neutral hydrogen emission. The contour levels are (− 1.5, 1.5, 2, 3, 4, 5, 6, 8, 10, 12, 14, 16, 18) mJy $beam^{-1}$. (1 mJy $beam^{-1}$ corresponds to 6.2×10^{19} cm^{-2} in each channel.) The beam is shown in the top left-hand corner of plane 24. Note that the anomalous velocity cloud is the north-western component. The crosses mark the optical positions of NGC 3227 and 3226.

The emission from the cloud was isolated by 'blanking' out the galactic disc emission (by the same process as described for the disc in Section 3.5). The range in velocity across the cloud, as measured from position–velocity slices is ~ 150 km s^{-1}, up to a maximum of ~ 1330 km s^{-1}. Moment analysis of the cloud revealed evidence for mild rotation; the velocity field can be seen in Fig. 8(c) and the integrated neutral hydrogen distribution in Fig. 8(a).

By studying both the positions and the velocities of the disc, cloud and northern plume, we hoped to establish the role played by the cloud in this complicated system. At first sight of the H I distribution, one might assume that the two tidal tails originate from the galactic disc. However, the high-resolution data shows that the velocity at the base of the northern plume corresponds more closely to the velocity of the cloud than to that of the disc.

There are a number of scenarios that might explain the 'cloud'. One possibility is that the cloud could be a gas-rich dwarf galaxy that is the interacting companion, instead of, or in addition to NGC 3226, and the northern plume has been 'pulled' out of this dwarf galaxy. There are a number of interacting systems of this nature where two galaxies interact and each develops one tidal tail (e.g. NGC 4676, 4038 and 4039, 2623, 2992 and 2993, Toomre & Toomre 1972). Indeed it is now becoming apparent that a hierarchy of such tidal interactions exists, with even star-forming dwarf galaxies showing

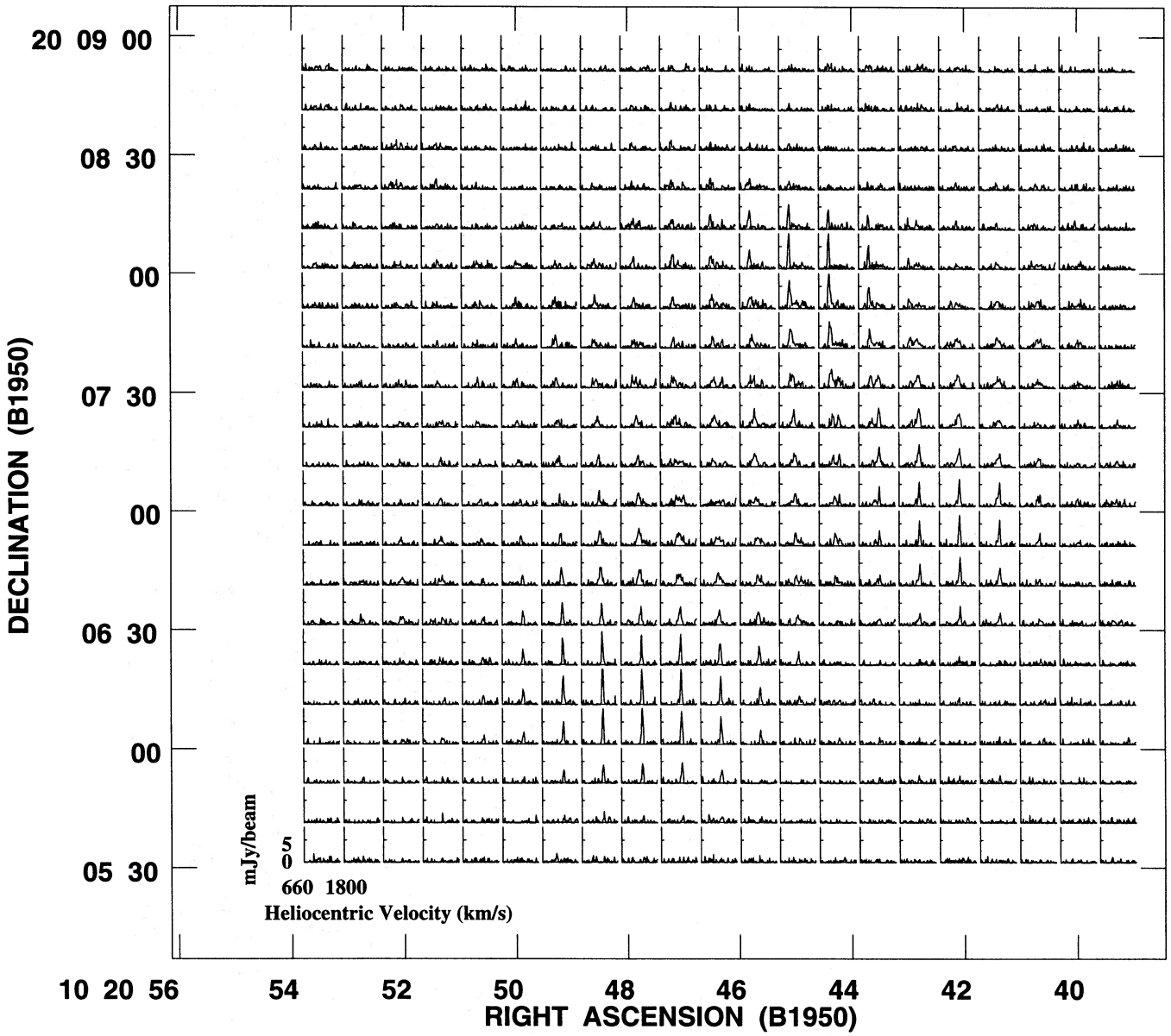

Figure 3. Grid of spectra, taken from the C-array data, showing emission across NGC 3227 and the anomalous velocity cloud. Only emission from every second pixel is plotted.

tidal plumes created as a consequence of interaction with lower mass companions (e.g. NGC 428, Smoker et al. 1995).

Another possibility is that this cloud is a product of the interaction between NGC 3226 and 3227 and has either condensed from the tidal-tail debris or was ejected during the interaction. In fact, optical and H I knots do seem to be another consequence of the merger phenomenon (Barnes & Hernquist 1992a,b), with a number of interacting galaxies exhibiting knots in their tidal tails (Schweizer 1978; Mirabel, Lutz & Maza 1991). It is thought that clumps of material, perhaps as large as dwarf irregulars, spheroids or full-size irregular galaxies, may be ejected during a tidal encounter (Hibbard et al. 1994) or self-gravity in the tails may be responsible for the creation of this small-scale structure.

One example of this is NGC 4038, 4039, in which Zwicky (1956) noticed a concentration of luminosity near the end of the southern tail and speculated that such objects might evolve into dwarf galaxies. The presence of the dwarf was also noted by van der Hulst (1979) from his neutral hydrogen observations, and Mirabel, Dottori & Lutz (1992) proposed a model for the formation of the dwarf irregular from the tidal remnants that were ejected during the interaction.

The mean velocity of the cloud, of ~ 1285 km s^{-1}, is only 150 km s^{-1} greater than the systemic velocity of NGC 3227. According to studies of dwarf galaxies and their environments (Vader & Chaboyer 1994) this small difference would suggest that the cloud is physically associated with NGC 3227 [a similar result was found for dwarfs associated with early-type giant galaxies, with velocity differences of less than 300 km s^{-1} for field galaxies (Vader & Chaboyer 1992)]. The flux integral over the 'cloud' is found to be 3.92 Jy km s^{-1},

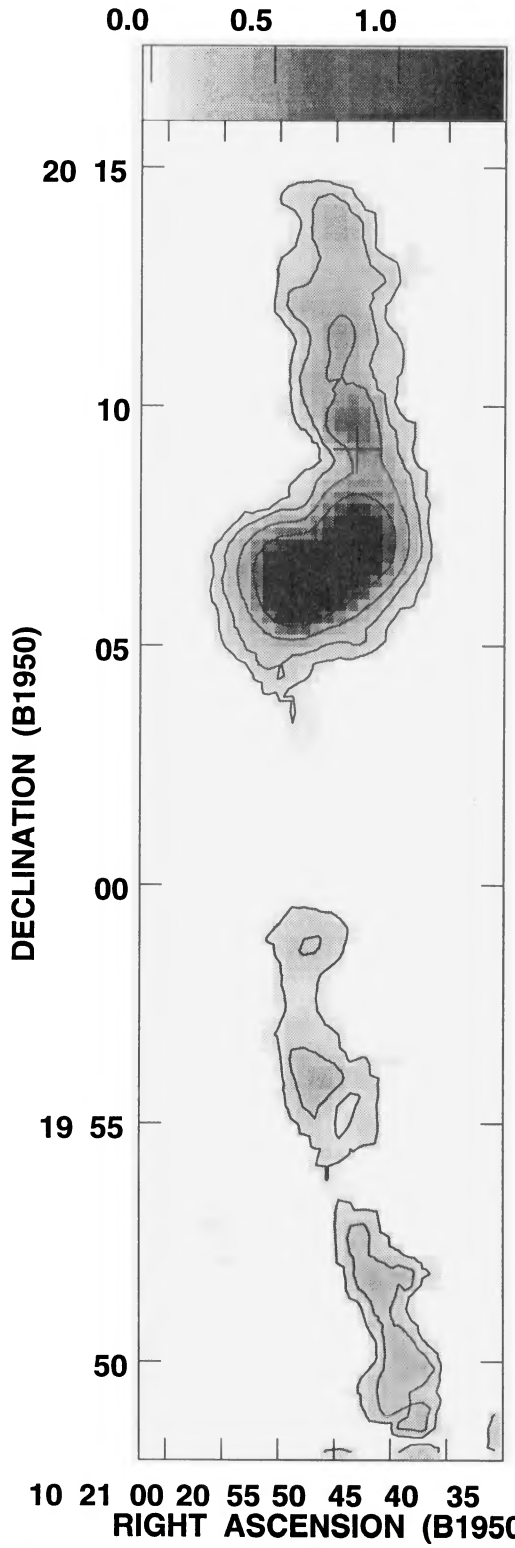

Figure 5. D-array neutral hydrogen distribution, integrated over the velocity range of 1243 to 1490 km s^{-1}, showing extensive tidal tails stretching away from the main body of NGC 3227. The position of the companion galaxy, NGC 3226, is marked as '+', at the base of the northern plume. Note: not *all* of the emission from the galactic disc of NGC 3227 is included here. The contour levels are (100, 200, 400, 800, 1600, 3200) mJy $beam^{-1}$ ms^{-1} and the beamsize is 60.74 × 58.15 arcsec. 100 Jy $beam^{-1}$ ms^{-1} corresponds to 3.2×10^{19} cm^{-2}.

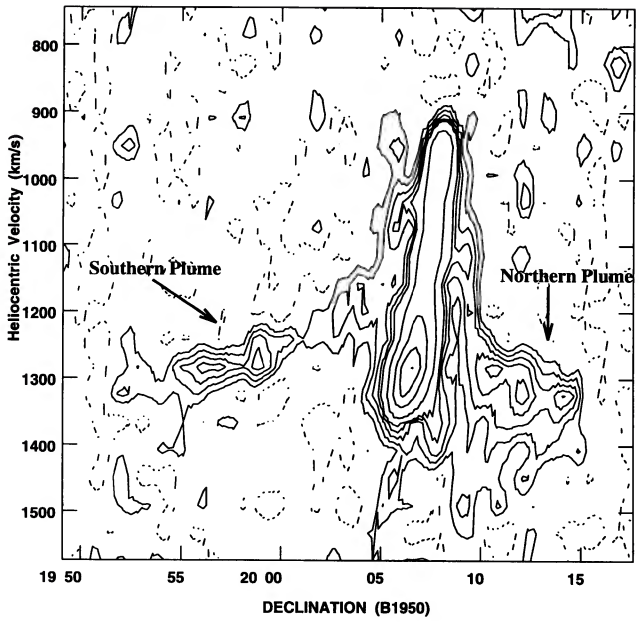

Figure 6. Position–velocity diagram of the region shown in Fig. 5. The data were summed over the RA axis and the contour levels are (−2.5, 2.5, 5, 7.5, 10, 12.5, 25, 50, 75, 100) per cent of the peak.

which gives a total H I mass of 2.1×10^8 $M_\odot$ if placed at the distance of NGC 3227 (15.1 Mpc). The diameter of the 'cloud' is 5.8 kpc, which is consistent with the sizes of dwarf galaxies, which lie typically in the range of 5–10 kpc. The inclination of the cloud is unknown, but, assuming that it is a circular disc, the total dynamical mass could lie in the range $3 \times 10^9 < M_T < 28 \times 10^9$ $M_\odot$.

3.5 The disc of NGC 3227

The D-array observations showed that complex dynamics existed, in the disc NGC 3227, in the form of double-peaked emission lines (Fig. 3). The C-array observations, however, easily resolved these complex motions into emission from the disc and that from the anomalous velocity cloud. As emission from the cloud was so easily separated from the galactic disc emission, we blanked out the cloud in order to examine the kinematics of the disc without contamination from the cloud motions. Emission from the cloud was blanked out from each channel in which it appeared and moment analysis was performed on the blanked cube. The resulting integrated neutral hydrogen emission (zeroth moment) from the disc can be seen in Fig. 8(a) along with the cloud, which was blanked out and superimposed in contours to indicate its position relative to the disc.

Surprisingly, the disc is really quite undisturbed and Figs 7 and 8(b) show its approximate solid-body rotation. The line of nodes bends over to the top right of the disc (Fig. 8b), which could be interpreted as warp of the disc. This would not be too surprising considering that the galaxy is involved in an interaction.

The mean integrated neutral hydrogen flux was measured from the zeroth-moment map [Fig. 8a and a neutral hydrogen mass of 5.7×10^8 $M_\odot$ for the disc was derived (after Roberts 1978)]. A value of 56 ± 4° for the inclination of the

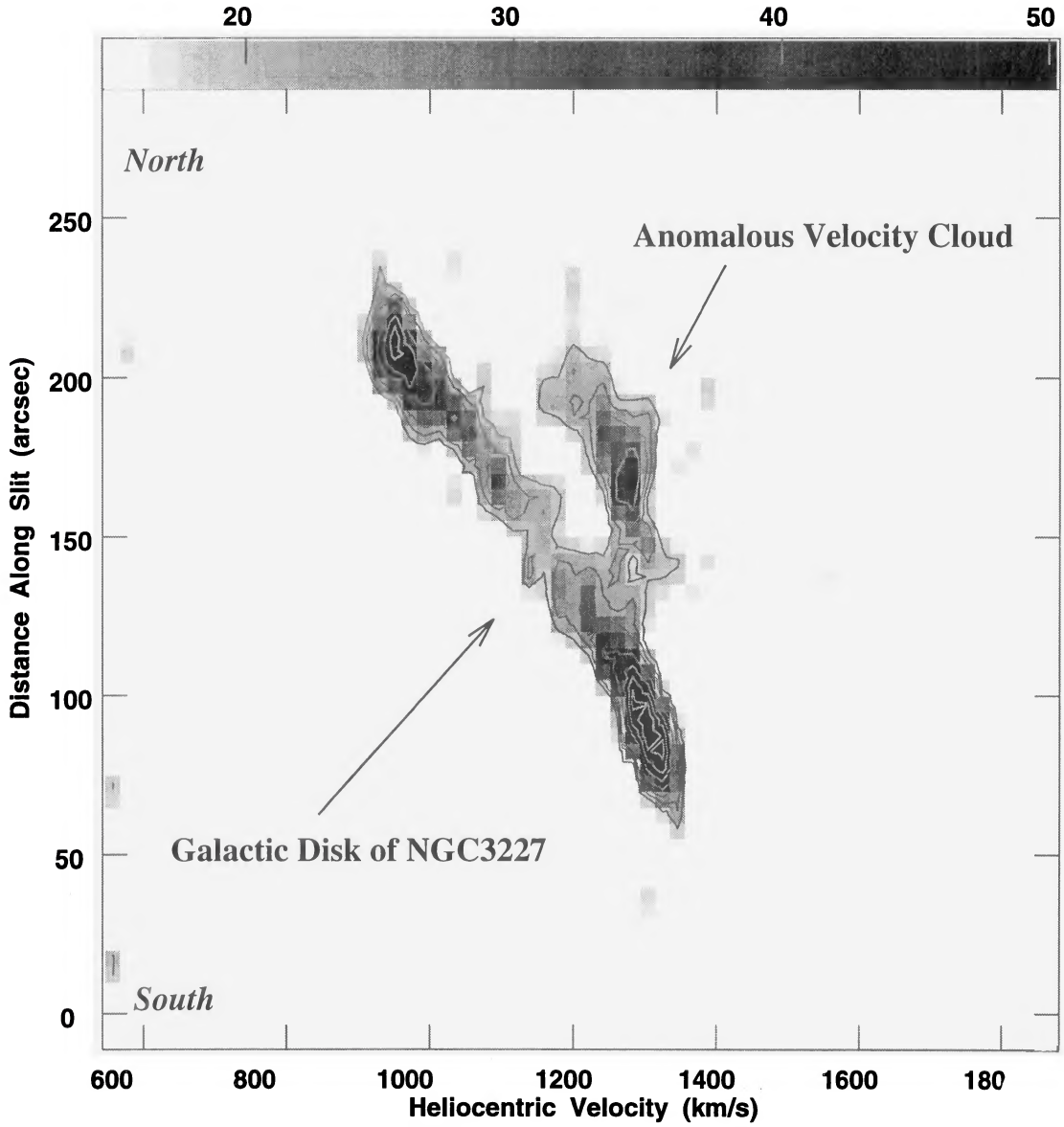

Figure 7. Position–velocity diagram formed by summing the emission parallel to the major axis along PA 158°. The origin corresponds to RA $\sim 10^h20^m52^s$, dec $\sim 20°05'00''$. The emission from the cloud and disc are indicated.

disc was derived from the major- to minor-axis ratio, measured from the 10 per cent contour level. It should be noted, however, that the H I distribution does not seem to be symmetrical about the major axis. This asymmetry may be because of the interaction and the presence of the cloud.

The total dynamical mass of 9.9×10^{10} $M_\odot$ was derived from the rotation curve (Fig. 9), assuming circular motions out to a radius of 95 arcsec. The rotation curve was derived by fitting a one-parameter rotation curve with constant velocity to a series of thin annuli from a radius of 10 out to 100 arcsec. In the fitting process the inclination of the disc was held fixed at 56°, but the systemic velocity and major axis PA were free to vary. Convergence of the solutions was achieved with values of 1135 ± 10 km s^{-1} for the systemic velocity and $158 \pm 2°$ for the major axis PA. The neutral gas close to the centre is disturbed and quite clearly exhibits non-solid-body motion with rapid changes in velocity in the central 20 arcsec (Fig. 10).

Heckman et al. (1978) performed a similar calculation using their single-dish observations and obtained a neutral hydrogen mass of 1.03×10^9 $M_\odot$ (corrected for $H_0 = 75$ km s^{-1}) and a total mass of 4.47×10^{11} $M_\odot$. However, they state that their value, of total mass, is an overestimate as they assumed circular motions out to 3 arcmin, where the H I is, in fact, highly disturbed.

3.6 The nuclear regions

Although the kinematics of the gas in the main disc of the galaxy are remarkably undisturbed, the integrated neutral hydrogen distribution shows evidence of a 'Z'-shaped bar of enhanced emission, crossing the nucleus in a north-west to

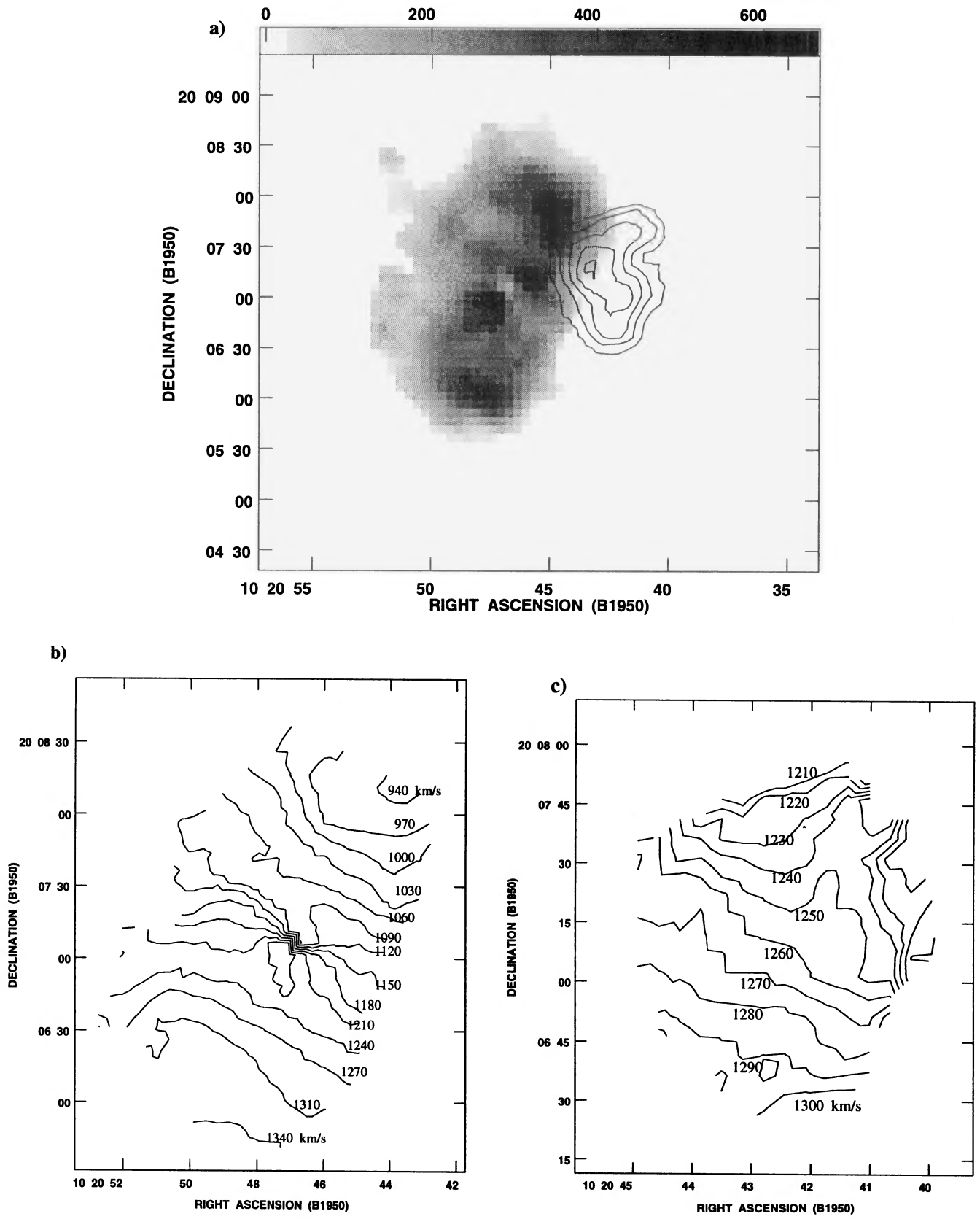

Figure 8. (a) Integrated neutral hydrogen emission (zeroth moment) from the disc of NGC 3227 is shown in grey-scale with the neutral hydrogen distribution of the cloud superimposed in contours. The contour levels are 100, 200, 300, 400, 500 Jy beam^{-1} ms^{-1} and 100 Jy beam^{-1} ms^{-1} corresponds to 3×10^{20} cm^{-2}. (b) The velocity field (moment 1) of the disc of NGC 3227 with isovelocity contours labelled in km s^{-1}. (c) The velocity field of the anomalous velocity cloud, with the contours labelled in km s^{-1}. The beamsize is 20.47×18.25 arcsec.

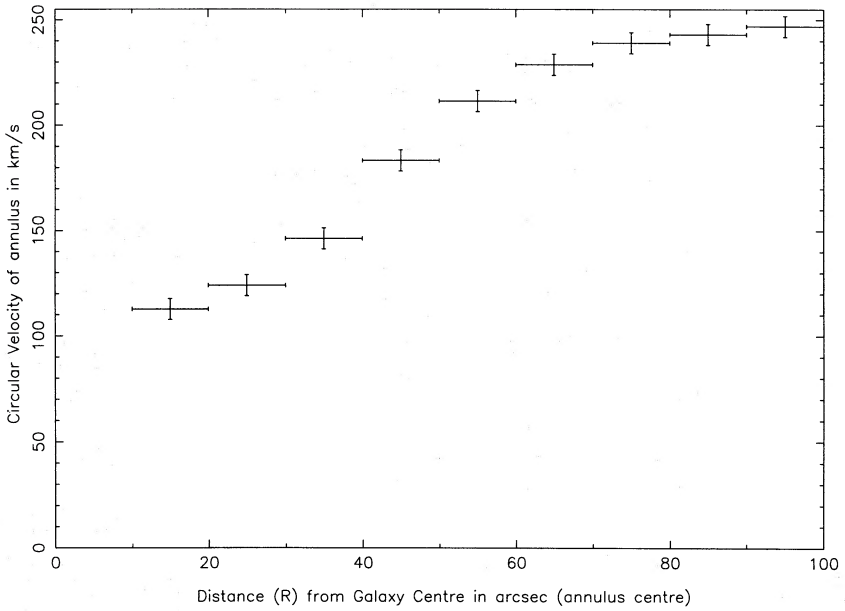

Figure 9. Rotation curve derived from annulus fitting.

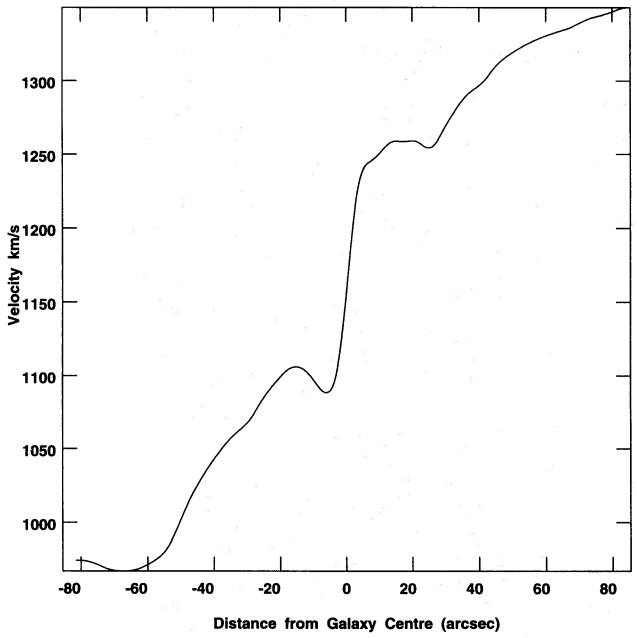

Figure 10. Slice across integrated H I velocity field, along the major axis. Note the rapid changes in velocity in the central 20 arcsec.

south-east direction. The 'arms' of the bar trail in the same sense as the optical spiral arms and the neutral hydrogen plumes.

Sundin, Donner & Sundelius (1993) have shown that, when a uniform disc is perturbed by a companion, a spiral pattern forms initially, which, with time, starts to disperse as a bar begins to form in the centre. Clearly, the interaction could have played a major role in the formation of the Z-shaped bar in NGC 3227. Equally we may speculate on the importance of this Z-shaped emission in fuelling the active nucleus. In the present observations, the absence of any evidence of high-velocity gas, significant tidal disruptions of the disc or tidally stripped gas being deposited directly on to the nucleus, leads us to the conclusion that the presence of the bar is crucial to the fuelling of the AGN.

Recently 'bars' have become a favoured mechanism for transporting material at larger radii towards the nucleus of a galaxy (Schwarz 1985; Combes & Gerin 1985; Athanassoula 1992; Barnes & Hernquist 1992; Shaw et al. 1993), with the possibility of inflowing gas (on kpc scales) accumulating in circumnuclear rings, bar-like features or 'spiral arms' (Athanassoula 1992; Vila-Viláro et al. 1994). It is unclear how the gas is driven further into the centre, to subparsec scales, to fuel the active nucleus, but Shlosman, Frank & Begelman (1989) have suggested small bars on the nuclear scale, i.e. 'bars within bars'. Forbes, Kotilainea & Moorwood (1994) suggest that the presence of molecular bars may be a necessary (although perhaps not sufficient) requirement for nuclear activity.

In the case of NGC 3227, it is interesting to examine the possible connections between the different nuclear components that have been observed. Meixner et al. (1990) have detected a small bar-like feature of CO (J = 1–0) emission in NGC 3227, approximately 17 arcsec in extent, crossing the nucleus in an approximately east–west direction. The structure of the CO bar suggests it may be a continuation of the H I bar (see Fig. 11). The two components in the CO image are also seen to straddle the optical nucleus and are in a PA that is ~perpendicular to the PA of the radio jet (Mundell et al. 1995b). In fact, Robinson et al. (1994) have argued that there is an intimate link between such bar-driven flows, the formation of molecular tori and the collimation of the ionizing radiation field of AGNs. If this is the case in NGC 3227, we may be seeing the presence of a molecular torus around the nucleus that is responsible for the collimation of the UV radiation that ionizes the [O III] wedge seen by Mundell et al. (1995b).

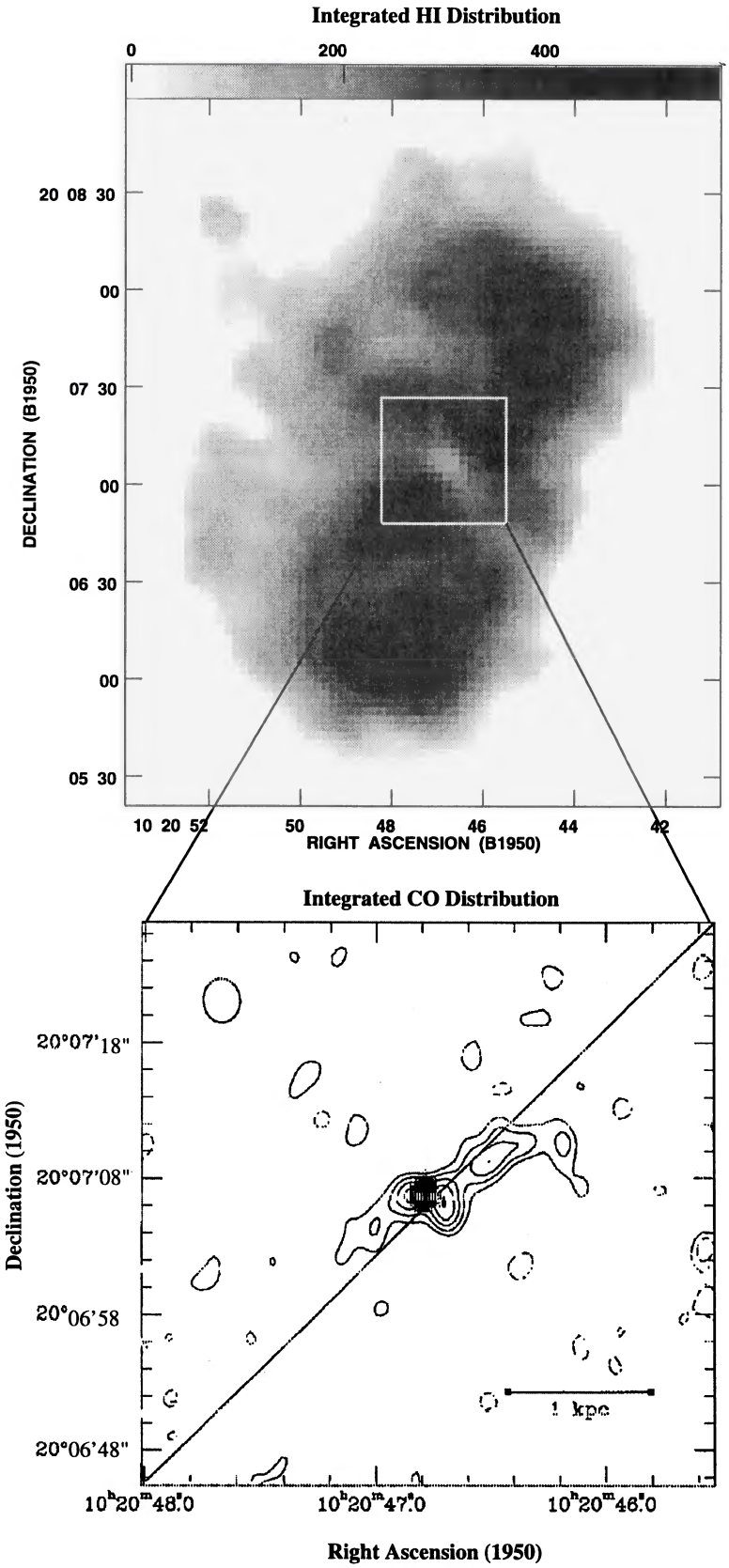

Figure 11. Grey image of the integrated H I distribution of NGC 3227's galactic disc; the white box indicates the region covered by the CO contour map below (Meixner et al. 1990). The CO bar appears to be a continuation of the H I bar.

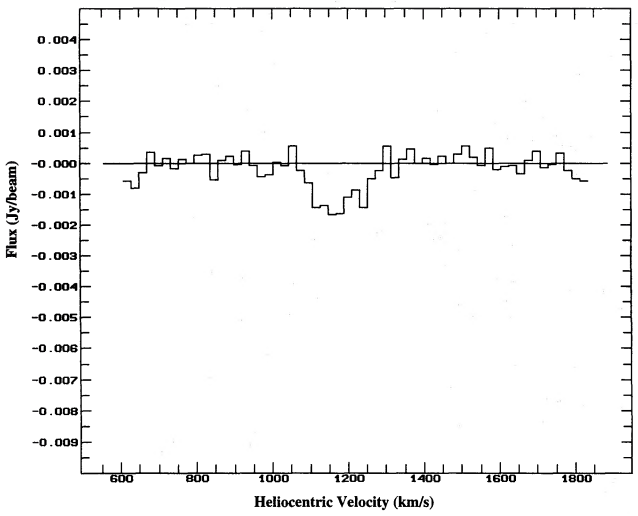

Figure 12. Neutral hydrogen absorption against the central brightest continuum pixel of NGC 3227, from the naturally weighted C-array data.

Emission from the neutral hydrogen bar can only be traced to within ~20 arcsec of the nucleus due to the resolution of the present observations and the presence of a 'hole' in the centre of the disc (see Fig. 8a).

We therefore subtracted the mean emission in the region from the central pixel (see Section 2.1) to reveal the absorption spectrum shown in Fig. 12. A Gaussian fit to the absorption feature gives a velocity centroid of ~1171 km s^{-1} and a width (FWHM) of ~134 km s^{-1}. The column density is 5.5×10^{20} cm^{-2} assuming a spin temperature of 100 K. Interestingly this compares well with the hydroxyl absorption feature detected by Rickard, Bania & Turner (1982). The OH absorption feature they detected in NGC 3227, using the Aricebo 305-m telescope with a 2.9-arcsec beam, is centred at 1137 km s^{-1} and has a width of 133 km s^{-1}.

Higher resolution observations are required to verify the presence of this absorption and to study, in detail, any smaller scale absorption structure that may be present against the radio continuum double component that was discovered with MERLIN (Mundell et al. 1995b). Similar to the interpretation suggested for the absorption of NGC 4151 (Mundell et al. 1995a), the absorption in NGC 3227 may be due to an obscuring torus around the active nucleus.

Observations at other wavelengths also suggest the presence of large amounts of neutral gas towards the nucleus. Rubin & Ford (1968) suggest a presence of large amounts of absorbing material in the nucleus, indicated by high $H\alpha/H\beta$ ratios, large mass to luminosity ratio, and similar velocities of the Na D line and the broad emission line. Meixner et al. (1990) also find that unresolved molecular gas concentrations imply an H_2 mass of 1.3×10^8 $M_\odot$ within a diameter of less than 150 pc.

4 CONCLUSIONS

We have observed the neutral hydrogen emission from the interacting Seyfert galaxy NGC 3227; we detect no H I emission from the companion galaxy NGC 3226.

We have detected two large tidal tails, extending ~31 kpc north and ~70 kpc south of the main body of NGC 3227, which provide strong evidence that NGC 3227 is involved in an interaction.

We have also discovered a rotating cloud of H I, situated at the base of the northern plume, which we suggest may be a gas-rich dwarf galaxy. This cloud may be one of the bodies responsible for the tidal disturbance of NGC 3227, or it may have formed as a consequence of the interaction between NGC 3227 and 3226.

We detect no high-velocity gas associated with NGC 3227, nor do we find evidence for the low-velocity gas reported by Heckman et al. (1978).

The galactic disc of NGC 3227 is in relatively undisturbed solid-body rotation.

We derive a total dynamical mass, for the disc, of 9.9×10^{10} $M_\odot$, fixing the inclination of the disc at 56° and assuming circular motions out to a radius of 95 arcsec. We deduce a value of 1135 ± 10 km s^{-1} for the systemic velocity of NGC 3227 and derive values of 56° and 158 ± 2° for the inclination and PA of the major axis respectively.

We see evidence for a bar in the H I distribution which seems to be a continuation of the CO bar.

The total neutral hydrogen mass in the NGC 3227 system is 1.1×10^9 $M_\odot$ with the mass being distributed between the components as follows: disc = 5.7×10^8 $M_\odot$; cloud or 'dwarf' = 2.1×10^8 $M_\odot$; northern plume = 1.8×10^8 $M_\odot$; southern plume = 1.3×10^8 $M_\odot$.

We see evidence for neutral hydrogen absorption against the radio continuum nucleus which is similar to that detected from OH absorption measurements.

ACKNOWLEDGMENTS

We thank Andy Robinson, D. J. Saikia and Dave Shone for helpful discussions, and Margaret Meixner for assistance with the CO image. We also thank the referee, Tim Heckman, for useful suggestions. NRAO is operated by Associated Universities, Incorporated, under co-operative agreement with the National Science Foundation.

REFERENCES

Adams T. F., 1977, ApJS, 33, 19
Athanassoula E., 1992, MNRAS, 259, 345
Baars J. W. M., Genzel R., Pauliny-Toth I. I. K., Witzel A., 1977, A&A, 61, 99
Barnes J. E., Hernquist L., 1992, ARA&A, 30, 705
Blitz L., Mathieu R. D., Bally J., 1986, ApJ, 311, 142
Borne K. D., Richstone R. O., 1991, ApJ, 369, 111
Bushouse H. A., 1986, AJ, 91, 255
Clements E. D., 1981, MNRAS, 197, 829
Combes F., Gerin M., 1985, A&A, 150, 327
Dahari O., 1984, AJ, 89, 966
Dahari O., 1985, ApJS, 57, 643
Edelson 1987, ApJ, 313, 651
Forbes D. A., Kotilainen J. K., Moorwood A. F. M., 1994, ApJ, 433, L13
Gallagher J. S., Knapp G. R., Faber S. M., 1981, AJ, 86, 1781
Haynes M. P., Giovanelli R., Chincarini G. L., 1984, ARA&A, 22, 445
Heckman T. M., 1978, PASP, 90, 241
Heckman T. M., Balick B., Sullivan W. T., 1978, ApJ, 224, 745

Hibbard J. E., Guhathakurta P., van Gorkom J. H., Schweizer F., 1994, AJ, 107, 67
Högbom J. A., 1974, A&AS, 15, 417
Keel W. C., Kennicutt R. C., Hummel E., van der Hulst J. M., 1985, AJ, 90, 708
MacKenty J. W., 1989, ApJ, 343, 125
MacKenty J. W., 1990, ApJS, 72, 231
Meixner M., Puchalsky R., Blitz L., Wright M., Heckman T., 1990, ApJ, 354, 158
Mirabel I. F., Lutz D., Maza J., 1991, A&A, 243, 367
Mirabel. I. F., Dottori H., Lutz D., 1992, A&A, 256, L19
Mundell C. G., Pedlar A., Baum S. A., O'Dea C. P., Gallimore J. F., Brinks E., 1995a, MNRAS, 272, 355
Mundell C. G., Holloway A. J., Pedlar A., Meaburn J., Kukula M. J., Axon 1995b, MNRAS, 275, 67
Osterbrock D. E., 1991, ASP, 103, 874
Pedlar A., Howley P., Axon D. J., Unger S. W., 1992, MNRAS, 259, 369
Rickard L. J., Bania T. M., Turner B. E., 1982, ApJ, 252, 147
Roberts M. S., 1975, in Sandage A., Sandage M., Kristian J., eds, Galaxies and the Universe, Vol. 9, 309
Robinson A., Axon D. J., Perez E., Vila-Vilaró B., 1994, in Ward M. J., ed., Evidence for the Torus. Oxford Astrophys. Workshop, Oxford
Rots A. H., 1978, AJ, 83, 219
Rubin V. C., Ford W. K., 1968, ApJ, 154, 431
Salamanca I. et al., 1994, A&A, 282, 742
Shlosman I., Frank J., Begelman M. C., 1989, Nat, 338, 45
Schwartz M. P., 1985, MNRAS, 187, 73P
Schwartz M. P., 1985, MNRAS, 212, 677
Schweizer F., 1978, in Berkhuijsen E. M., Wielebinski R., eds, Structure and Properties of Nearby Galaxies. Reidel, Dordrecht, p. 279
Shaw M. A., Combes F., Axon D. J., Wright G. S., 1993, A&A, 273, 31
Simkin S. M., Su H. J., Schwarz M. P., 1980, ApJ, 237, 404
Smith B. J., Wallin J. F., 1992, ApJ, 393, 544
Smoker J. V., Davies R. D., Axon D. J., Hummel E., 1995, MNRAS, submitted
Sundin M., Donner K. J., Sundelius B., 1993, A&A, 280, 105
Toomre A., Toomre J., 1972, ApJ, 178, 623
Vader J. P., Chaboyer B., 1992, PASP, 104, 57
Vader J. P., Chaboyer B., 1994, AJ, 108, 1209
van der Hulst J. M., Rots A. H., 1981, AJ, 86, 1775
van der Hulst J. M., 1979, A&A, 71, 131
Vila-Vilaró B. et al., 1994, A&A, 302, 58
Zwicky F., 1956, Ergebnisse der Exakten Naturwissenschaften, 29, 344